

ELECTROMAGNETIC ACTUATOR OF A GENTLE PUMP MECHANISM FOR BLOOD TRANSPORT

S. Pech, H. Rathmann, R. Richter, T. Nagel, J. Lienig

Dresden University of Technology, Institute of Electromechanical and Electronic Design (IFTE), Helmholtzstraße 18, 01062 Dresden, sebastian.pech@outlook.com

ABSTRACT

The maximum operation time in blood pump applications is limited by blood damage caused by mechanical stress within the pump. To overcome this limitation, a new pumping principle is introduced. It is based on wave propagation inside a flexible tube in combination with positive displacement. The tube stimulation is generated by an electromagnetic actuator. In contrast to common roller pumps, it is possible to achieve a pumping operation without a complete tube occlusion. This ensures gentle pumping without damaging the blood cells. Our measurement of the pump curve and the trajectory of the shock head confirms the pumping operation without complete tube occlusion.

Index Terms - blood pump, hose pump, wave propagation, electromagnetic actuator

1. INTRODUCTION

The human heart is running through 2.7 billion working-cycles in its lifetime [1]. In this period, between 400 and 500 million liters of blood are pumped through the ventricles [1]. Today cardiovascular diseases are a widespread problem all over the population. If the heart is not able to pump a sufficient amount of blood anymore, a heart surgery or the use of extracorporeal circulation systems are the usual possibilities. In both cases, extracorporeal blood pumps, like roller pumps or centrifugal pumps, are used. When extracorporeal circulation systems are applied, the respiratory and circulatory functions of the patient organism are supported or completely replaced. A characteristic extracorporeal blood circulation is shown in Fig. 1.

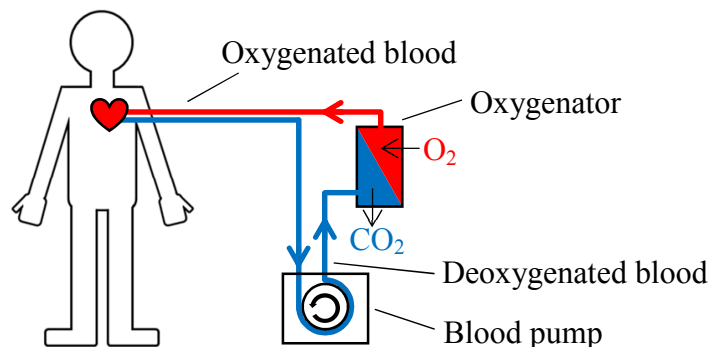


Fig. 1: Extracorporeal circulation

Typical applications of extracorporeal circulation are extracorporeal life support (ECLS) and extracorporeal membrane oxygenation (ECMO). In both cases, gas exchange is implemented by an oxygenator perfused with blood. A blood pump is used to perfuse the oxygenator and to run the circulation.

Within both components, the mechanical stress, the influence of external surfaces and the thrombosis damage the blood cells [2], [3]. The so-called hemolysis is the most important damage mechanism. Caused by the mechanical stress of the blood pump, the red blood cells (erythrocytes) are injured or destroyed. Consequently they cannot transport gas anymore. Due to these side effects, the application time for extracorporeal circulation is limited.

Depending on the application time, typical blood pumps are roller pumps (peristaltic pumps) and centrifugal pumps. Roller pumps consist of a flexible tube, a housing and a rotating part occupied with rollers. They belong to the category of peristaltic pumps and are typically used for life-support-machines and dialysis treatment. During operation, the rotating rollers squeeze the flexible tube. This occlusion causes hemolysis and abrasion of the tube material. Therefore the application time of roller pumps is limited to several hours only.

Centrifugal pumps are the second common used pump type for these applications. They are typical flow-machines. In contrast to roller pumps, centrifugal pumps are not self-priming. A fast rotating impeller accelerates the blood which is flowing out of the exit of the pump. Due to the high velocity gradient inside the pump, high mechanical stress is implemented into the blood [4], resulting in hemolysis too. Typical application times of centrifugal pumps are several days.

To increase the application time of blood pumps, a novel gentle pump mechanism is needed to reduce the blood damage. We propose a non-occlusive method to reduce the mechanical stress to the red blood cells. Furthermore, we aim for avoiding the direct contact between the fluid and moving parts like in centrifugal pumps to decrease the external surface coming in contact with the blood. The introduced pump mechanism is also designed without valves to avoid additional blood damage. For a safe practical application, our goal is to achieve a maximum flow rate of 5 l/min and a maximum back pressure of 50 kPa.

2. PUMPING PRINCIPLE

2.1 Functional model

The presented pumping mechanism is based on coupling of mechanical oscillation into a flexible tube. The functional model of the pump is shown in Fig. 2. It shows how the energy flow (blue, solid), the information flow (red, dash dot) and the material flow (green, dash) are transformed by the pump.

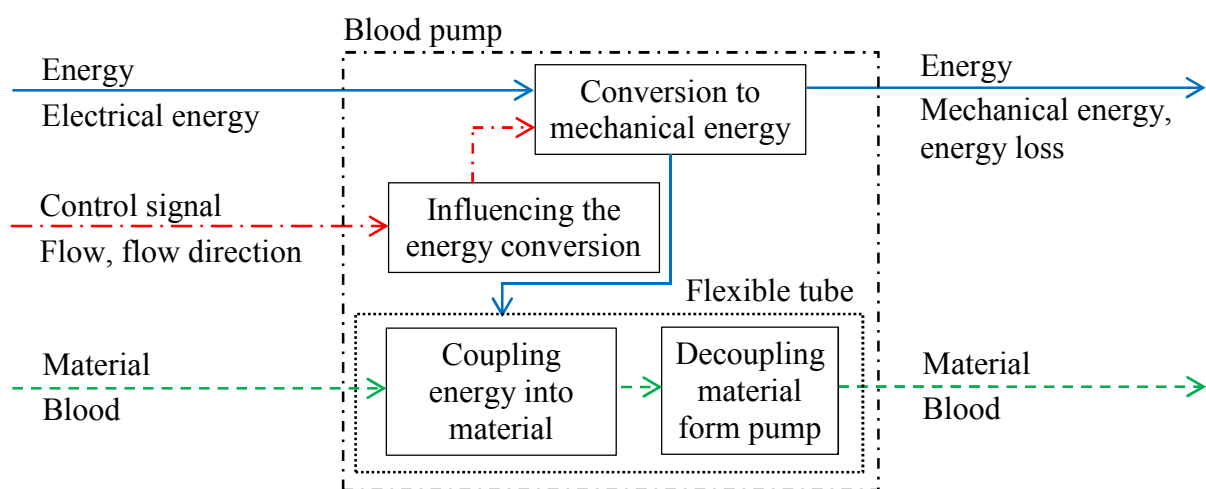


Fig. 2: Functional model of the blood pump

The three model inputs are the energy flow in form of electrical energy, the information flow in form of the control signal and the material flow represented by the blood flow. Influenced by the control signal, the electrical energy is converted into mechanical energy. In the next step, this is coupled into the flexible tube and the therein located blood. After the energy transfer, the blood is decoupled for the pump.

2.2 Part 1: Wave propagation

It is supposed, that one part of the pumping mechanism is based on wave propagation within the flexible tube by coupling of micro oscillations. A similar pumping mechanism is known as impedance pump. Fig. 3 shows a typical assembly of an impedance pump and its operation.

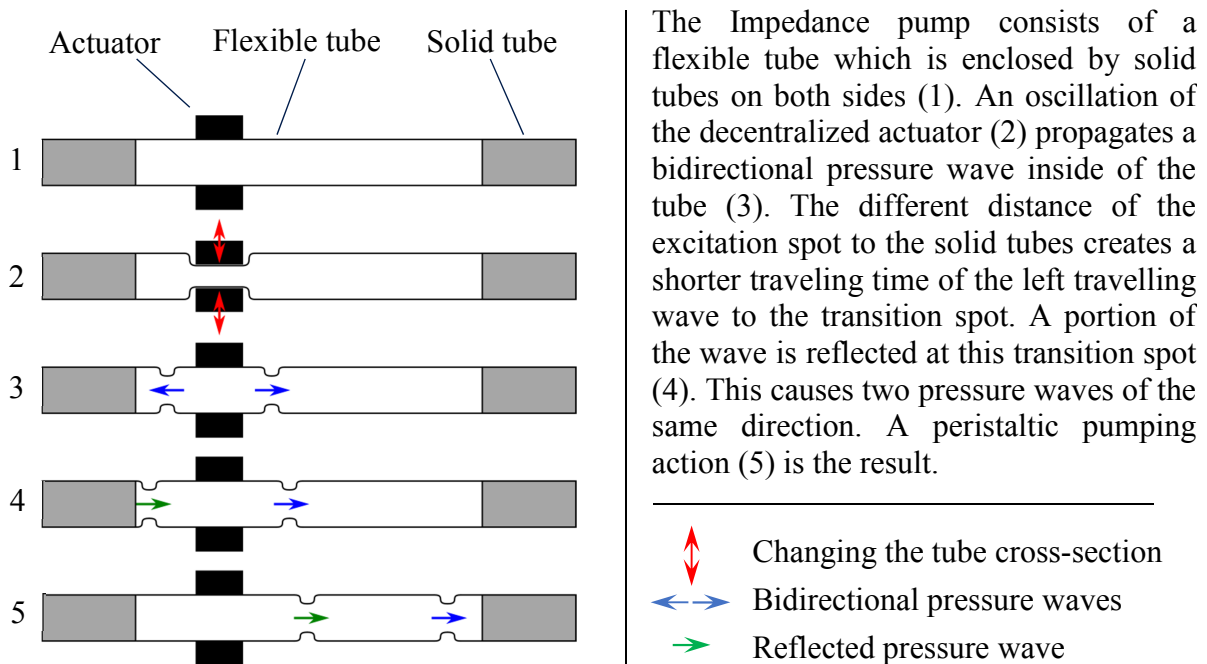


Fig. 3: Functional principle of an impedance pump, according to [5]

Frequencies about (1 ... 8) Hz and amplitudes about 100 % of the tube diameter [5] are usual during the operation of the impedance pump. In contrast to that, the presented pumping mechanism typically works with higher frequencies and smaller amplitudes to ensure a gentle fluid transport. Furthermore the flexible tube is stimulated at several spots. In this way it is possible to push the wave along the tube. To achieve this, the use of a rotationally symmetrical actuator arrangement with at least one tube winding is advantageous. Circulating shocks impact on the tube and stimulate the forming of waves in the fluid. While shocking the flexible tube bidirectional waves are propagated similar to the impedance pump (according to Fig. 3, Step 3). In contrast to the impedance pump there is no reflection of the returning wave (the wave which is traveling against the pumping direction) since there is no transition spot. By superimposition of the returning and the leading wave, the actual pumping direction is given by the direction of the circulating shocks [6].

In Fig. 4 the chronological sequence of this wave propagation is shown. The arrangement consists of four stimulation spots which are allocated symmetrical around one tube winding. Clockwise circulating shocks (red colour) with the frequency of $f = 1/T$ are stimulating the tube. Different arrows are marking the leading wave (blue colour) and the returning wave (green colour). These waves are driven by the amount of shocks (numbers besides the arrows) which impacts them while passing the stimulation spots and simultaneous stimulation. It can

be seen that the leading wave is getting more powerful by every impact because it has the same direction like the circulating shocks. To ensure this, the propagation speed of the wave has to be tuned to the frequency of stimulation.

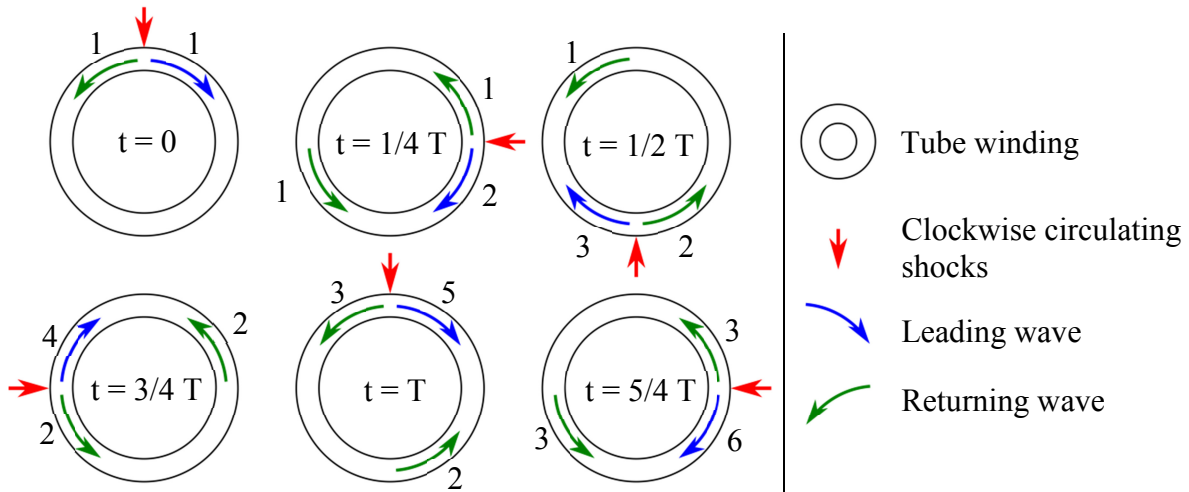


Fig. 4: Scheme of wave propagation inside of one tube winding

2.3 Part 2: Positive displacement principle

The second part of the pumping principle is based on positive displacement. Additionally to the shocks there is a positive offset of the tube stimulation. A shock head is coupling the stimulation into the flexible tube. As an example, the radial movement of the shock head is plotted in Fig. 5. The shocks are superimposed with an offset. Finally, the rotationally symmetrical actuator generates a continuous tube contraction. In contrast to common roller pumps the tube diameter is squeezed in radial direction just a view percent to avoid hemolysis, see Fig. 6. Because of this non-occlusive method there is a reverse flow inside of the tube. By increasing the frequency of the shock head, the reverse flow becomes lower than the flow in direction of the circulating shocks. In contrast to that, the typical occlusion of roller pumps is represented in Fig. 7. These pumps operate with complete occlusion and lower frequencies.

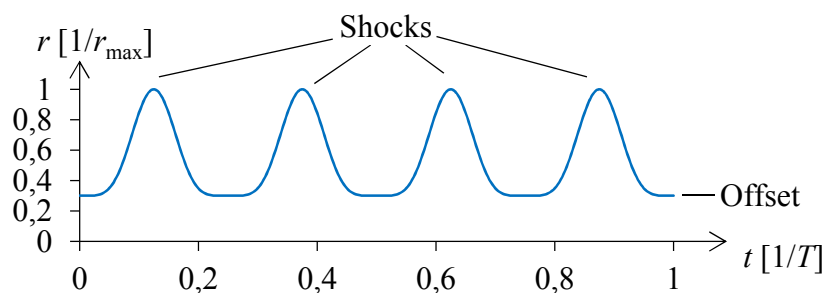


Fig. 5: Tube stimulation with four shocks per period and offset

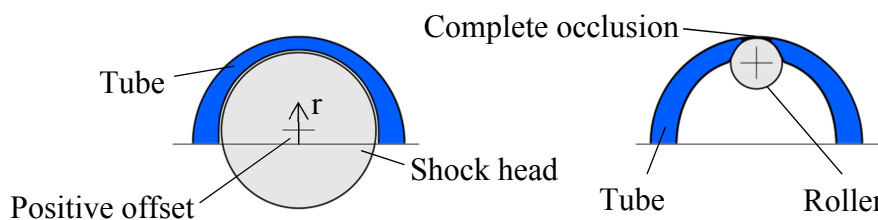


Fig. 6: Positive offset of the rotationally symmetrical actuator

Fig. 7: Typical occlusion of a roller pump

3. ACTUATOR

To implement the described principle, a pumping section is required. Its primary function is to stimulate the tube according to Fig. 5 and Fig. 6. The scheme of the actuator movement based on the rotationally symmetric design is shown in Fig. 8.

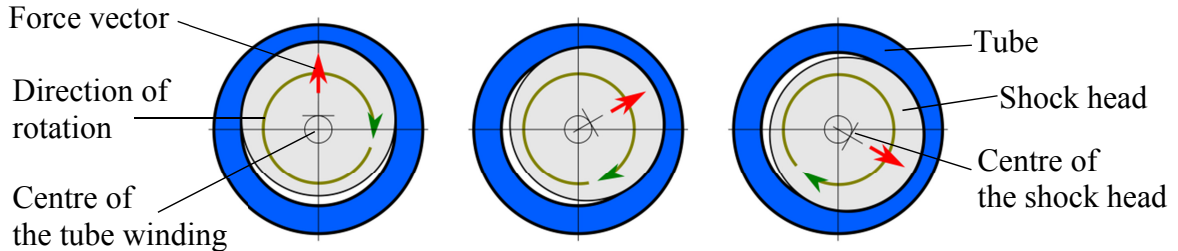


Fig. 8: Scheme of the rotationally symmetric pump section

Caused by a circulating force vector (arrow in red colour) the shock head moves synchronous to this (arrow in green colour) and the tube is squeezed. In this process the shock head is mounted without radially bearings. In this way, it can perform an eccentric movement referred to the centre of the tube winding.

To drive the pumping section, an electromagnetic actuator is required. A simple way to achieve the circulating force vector is the arrangement of six rotationally symmetric coils with a closed iron core as stator [7], [8]. The scheme of the cross-section of this actuator is shown in Fig. 9. Inside of this stator a rotor is enclosed. Between the stator and rotor, there is an air gap which creates the force vector and provides the space for the eccentric rotor motion. Furthermore it is important to avoid a collision between the rotor and the stator. The rotor is directly mounted on the shock head to transfer the force to the pump section. In Fig. 10 the scheme of the longitudinal section of the pump is illustrated [9]. The assembly consists of a stacked mounting of the pumping section and the actuator. Inside the pump section the tube windings and the shock head are placed.

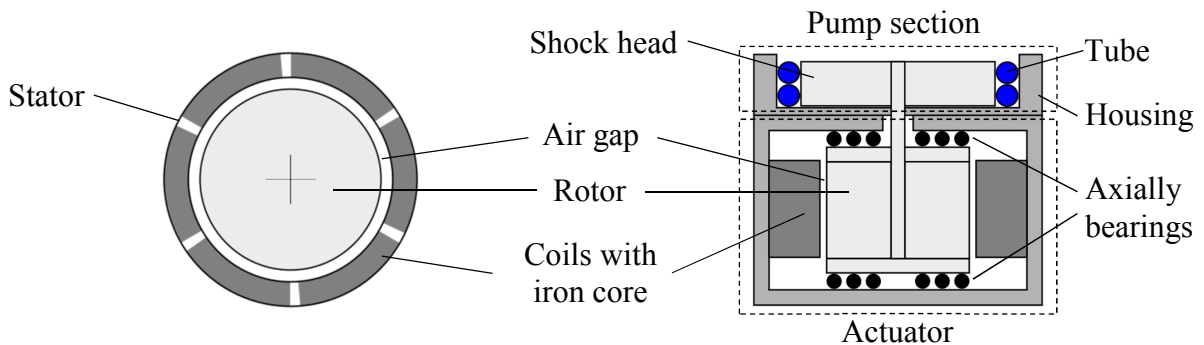


Fig. 9: Cross-section of the actuator according to [7], [8]

Fig. 10: Longitudinal section of the pump according to [9]

To avoid a tilt of the moving parts of the actuator, the rotor and the shock head is mounted with two axially bearings. Therefore the rotor can only perform a translational movement in radial direction and a rotation around its axis. In this way it is possible to separate the pumping section from the actuator to prevent a thermal coupling of the electromagnetic actuator and the fluid inside of the tube. The required circulating force vector is generated by a phase shifted coil current. This results in a periodic movement of the rotor. Due to the close

adaption of the rotor, the flexible tube and the housing, a roll off motion results and the rotor rolls off of the tube. In this way the described pumping principle is implemented.

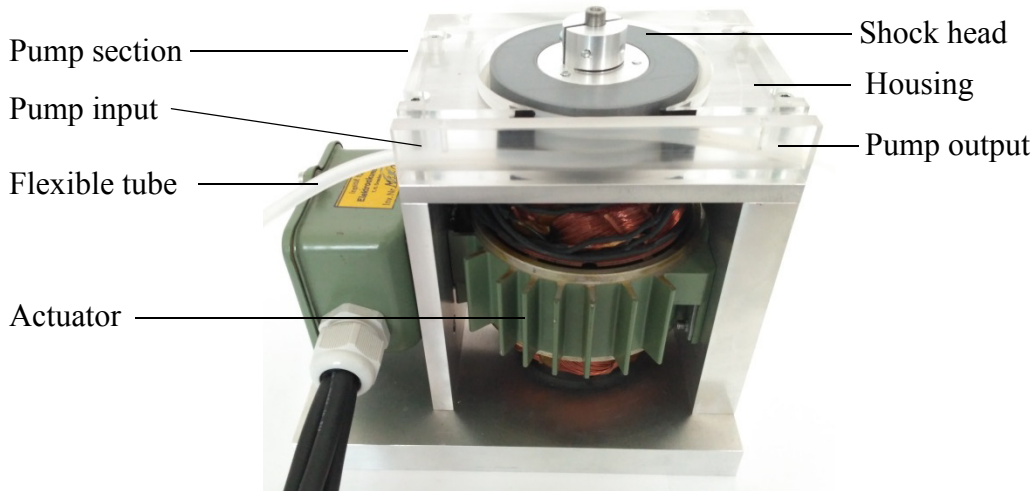


Fig. 11: Experimental setup of the pump

Fig. 11 illustrates the experimental setup of the pump. In the pump section, the tube is placed between the shock head and the housing. On the left side of the housing the pump input is placed. After three tube windings the tube leaves the pump section on the right side. In this way it is possible to decouple the fluid out of the pump.

4. PUMPING

In this part the measured pump curve is presented. A silicon tube with an inner diameter of $d_{tube_i} = 3$ mm and an outer diameter of $d_{tube_o} = 6$ mm is used for the experiments. The pump section is characterized by the diameter of the shock head $d_{sh} = 83.2$ mm and the inner diameter of the housing is $d_h = 94$ mm. In this setting the tube is applied with a positive offset of $t_{off} = 0.6$ mm according to equation (1). That means the resulting inner diameter of the tube is about 2.4 mm (80% of the initial state or 20% pre-squeezed) by assuming a linear occlusion of the tube.

$$r_{off} = d_{tube_o} - \frac{d_h - d_{sh}}{2} \quad (1)$$

For all experiments, the six coils are driven by a 3 phase power supply with a current amplitude of $\hat{i} = 1,74$ A and a frequency of $f = 75$ Hz.

4.1 Material and Methods

The presented pump curve is measured by using a flow sensor (BOITECH, VZS-005-VA [10]) and a pressure sensor (Honeywell, 40PC015G [11]) in combination with a data acquisition card (National Instruments, NI USB-6009 [12]). During the operation of the pump with water, the back pressure is adjusted hydrostatically or by a throttle valve. A constant back pressure is ensured by using an overflow-hopper. If the constant back pressure is reached, the flow measurement is started. In the next 10 s the flow rate Q and the back pressure p are measured and the mean value is calculated. To avoid interferences, the pressure sensor is placed behind the flow sensor. After acquisition of a single data point, the flexible tube is placed new in the pumping section.

4.2 Results

Fig. 12 shows the back pressure p as a function the flow rate Q . Until a back pressure of 20 kPa, the back pressure is adjusted hydrostatically (data points plotted by crosses). Above 20 kPa it is adjusted by using a throttle valve (data points plotted by squares). The results of the experiment show, that for the same back pressure the measured flow rate Q variates in a certain range. It is not possible to measure more accurate flow rates with the experimental setup of the pump. Probably the bearing of the moving parts (rotor and shock head) and the changing position of the flexible tube inside the pump section are the reasons for this behaviour.

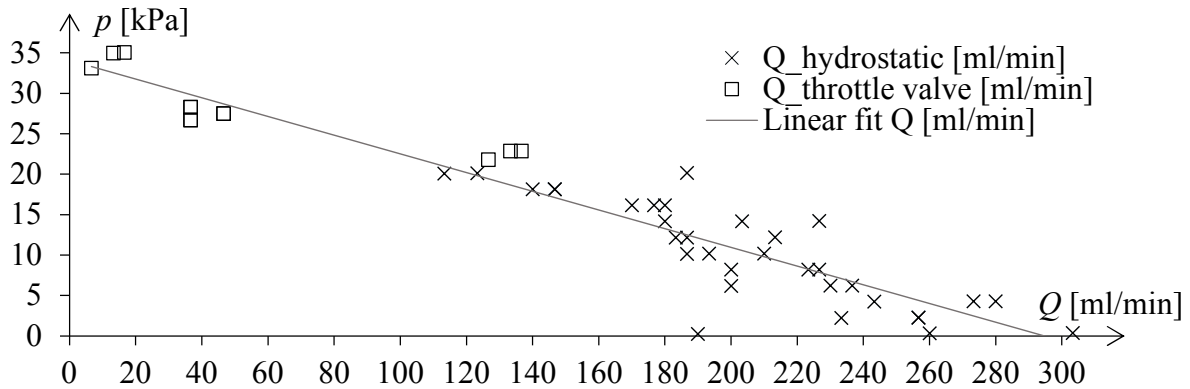
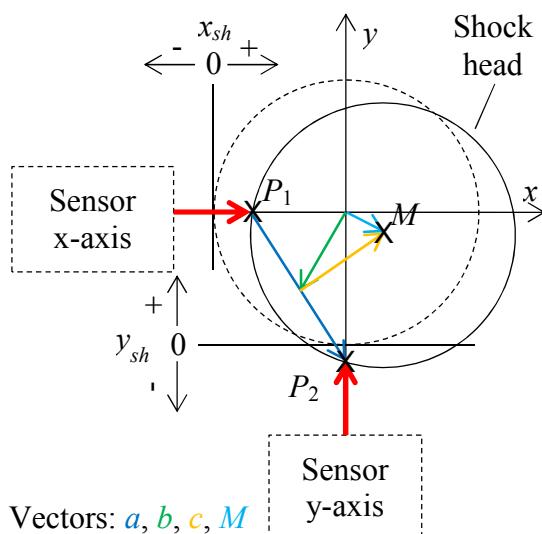


Fig. 12: Measured pump curve of the experimental setup with $f = 75$ Hz and $\hat{i} = 1.74$ A

As a result of the experiment, a linear fit can be placed to the acquired data points. Within the experiment a maximum back pressure of $p_{\max} \approx 34$ kPa and a maximum flow rate of $Q_{\max} \approx 295$ ml/min can be measured.

5. TRAJECTORY

To verify the amplitude of the tube stimulation an investigation of the shock head trajectory is needed. Two laser distance sensors (Wenglor, CP08MHT80 [13]) are used to record the trajectory. The measuring method is described in Fig. 13. The position of the centre of the shock head M can be determined by measuring the distances x_{sh} and y_{sh} by combining the vectors a , b and c .



Vectors: a , b , c , M

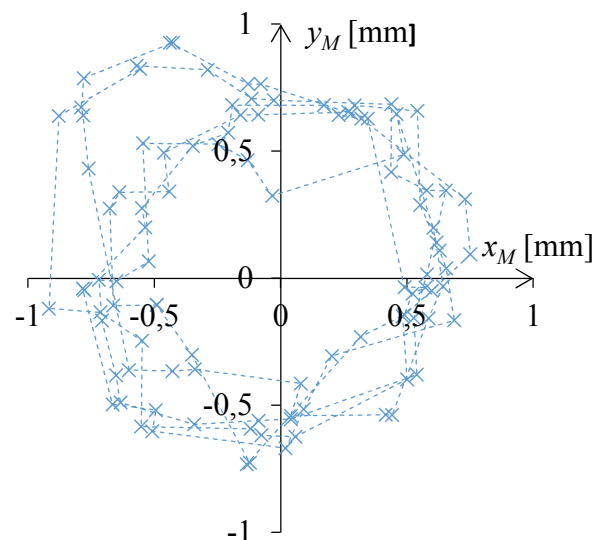


Fig. 13: Measurement of the shock head position

Fig. 14: Trajectory of the shock head at $f = 75$ Hz, measuring time 100 ms

In Fig. 14 the trajectory of the shock head is plotted exemplary. Within the measuring time of 100 ms the shock head executes about 4-5 periodic motions. An asymmetrical motion regarding to the centre of the trajectory ($x_{sh} = y_{sh} = 0$) is noticeable. Probably this is another reason for the varying flow rate in Fig. 12. Furthermore, the shock head trajectory does not show shocks in its amplitude like described in Fig. 5. The reason for that is the non-pulsed power supply, which is used for the experiment.

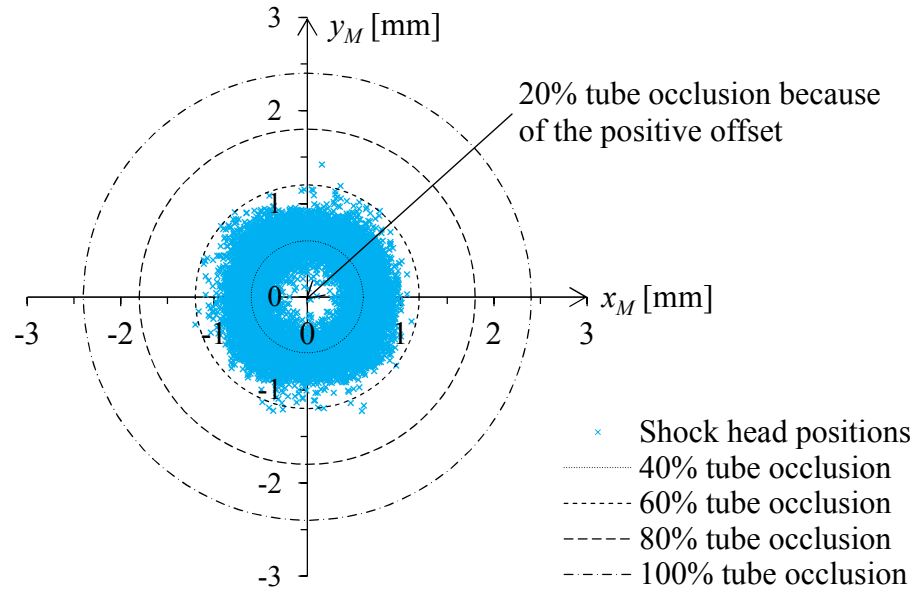


Fig. 15: Investigation of the tube occlusion, $f = 75$ Hz, measuring time 15s

In Fig. 15 the recorded shock head positions are plotted in blue colour. Due to the measuring time of 15 s, 15000 single shock head positions are shown. To validate the non-complete tube occlusion, circles of different tube squeezing states are plotted in different line styles in black colour. As already described in chapter 4, the tube is pre-squeezed to 20% in initial state. This corresponds to a trajectory amplitude of 0 mm (see arrow in Fig. 15). Concerning to that percentage, each circle describes a different tube squeezing percentage regarding to the inner diameter of the flexible tube $d_{tube_i} = 3$ mm. It can be seen, that the amplitude of the trajectory is always smaller than 1.2 mm. This means that the flexible tube is only squeezed about 60% regarding to the initial inner tube diameter. This proves that the flexible tube is not occluded completely during the pumping operation.

6. DISCUSSION

As described in the previous chapters there is a need for optimization to reach a more repeatable pumping operation. According to current knowledge the bearing of the moving parts must be improved to ensure a more symmetrical trajectory of the shock head. Another optimization point is to increase the maximum flow rate Q_{max} and the maximum back pressure p_{max} to reach the desired specification according to chapter 1. During the experiments, it has been advantageous for the pump operation to have an oscillating water column on the pump output. This fact confirms the pumping model of the impedance pump described in section 2.2. The shock head generates waves which are travelling along the water column. It is supposed, that constructive interferences support the pumping principle. For future applications a symmetrical trajectory of the shock head is important to ensure an even tube stimulation. This is the requirement for investigating the influence of the current amplitude \hat{i} and the frequency f of the power supply on the pumping behaviour. To improve the shocks stimulating the flexible tube, a pulsed power supply could be advantageous.

7. SUMMARY

We have introduced a novel pumping principle which is based on wave propagation in combination with positive displacement. As our experimental pump has shown, it is possible to generate a flow rate without a complete occlusion of the flexible tube. Hence, the described pumping principle has been demonstrated and validated. The measured pump curve shows variations in the flow rate Q at constant back pressures p which are traceable to the asymmetrical trajectory of the shock head and the bearing of the moving parts of the pump.

Further optimization of the actuator and regarding to the maximum values (Q_{max} and p_{max}) are necessary to use the pump for blood pump applications. In addition, the influence of the amplitude \hat{i} , shape and frequency f of the power supply on the pumping behaviour must be studied further. This should allow to implement controlled flow rates which can be used, for example, for pulsatile pumping operation or for implementing a dosing pump. Furthermore, the impact of the tube stimulation on the blood cells should be investigated.

After overcoming these limitations, a new pumping principle with significantly less blood damage will be available. It can increase the maximum operation time of blood pump applications and, hence, provide better therapy opportunities.

ACKNOWLEDGEMENT

This work is supported by the European Social Fund (ESF) and the Free State of Saxony.

REFERENCES

- [1] A. Fischer, Physiologie 6 Herz und Kreislauf, MEDI-LEARN Verlag, Marburg, 6. Edition, 2014.
- [2] D. Arora, M. Behr, M. Pasquali, Blood damage measures for ventricular assist device modelling. Moving Boundaries VII-Computational Modelling of Free and Moving Boundary Problems, WIT Press, Southampton, pp.129–138, 2003.
- [3] H.-D. Polaschegg, Red Blood Cell Damage from Extracorporeal Circulation in Hemodialysis, Seminars in Dialysis, Wiley-Blackwell, Oxford, Vol. 22, No. 5, pp. 524-531, 2009.
- [4] K. H. Fraser et al., A Quantitative Comparison of Mechanical Blood Damage Parameters in Rotary Ventricular Assist Devices: Shear Stress, Exposure Time and Hemolysis Index, Journal of Biomechanical Engineering, ASME, Vol. 134, No. 8, pp. 081002, 2012.
- [5] A. Hickerson, D. Rinderknecht, M Gharib, Experimental study of the behavior of a valveless impedance pump, Experiments in Fluids, Springer, Heidelberg, Vol. 38, No. 4, pp. 534-540, 2005.
- [6] M. Peschel, F. Breitenecker, Kreisodynamik, Akademie-Verlag, Berlin, 1990, ISBN: 3-05-500703-4.
- [7] A.-R. Druschke, M. Peschel, M. Schwaar, Elektromechanische Wandler nach dem Wanderfeldprinzip und ihre Anwendungsmöglichkeiten insbesondere in der Medizintechnik, messen-steuern-regeln, Verl. Technik, Vol. 23, No. 8, pp. 432-435, 1980.

- [8] A.-R. Druschke, M. Peschel, Patent DD156386C2, Elektrisch betriebene Pumpe, (1981-02-13), 1988-02-17.
- [9] S. Pech et al., Reference No. 10 2017 114 950.3, Elektrisch betreibbare Schlauchpumpe, Registered at DPMA on 2017-07-05.
- [10] B.I.O-Tech e.K.: VZS-005-VA, URL: <http://www.btflowmeter.com/fileadmin/PDF/Volumenzaehler/92202911-VZS-005-VA.pdf>, visited on 17-07-12.
- [11] Honeywell: 40PC015G, URL: https://sensing.honeywell.com/index.php?ci_id=138832, visited on 17-07-12.
- [12] National Instruments: NI USB-6009, URL: <http://www.ni.com/pdf/manuals/375296a.pdf>, visited on 17-07-12.
- [13] Wenglor sensoric GmbH: CP08MHT80, URL: https://www.wenglor.com/fileadmin/functions/wdm.php?dfile=CP08MHT80.PDF&pfad=fileadmin/download/DATA_SHEETS/EN/&sfile=Data_sheet_CP08MHT80.pdf&zip=false, visited on 2017-07-13.

CONTACTS

Dipl.-Ing. S. Pech	sebastian.pech@outlook.com
Dipl.-Ing. H. Rathmann	heiko-rathmann@web.de
Dr.-Ing. R. Richter	rene.richter@tu-dresden.de
PD Dr.-Ing. T. Nagel	thomas.nagel@tu-dresden.de
Prof. Dr.-Ing. habil. J. Lienig	jens.lienig@tu-dresden.de